

# A model to non-uniform Ni Schottky contact on SiC annealed at elevated temperatures

G. Pristavu,<sup>1</sup> G. Brezeanu,<sup>1</sup> M. Badila,<sup>1</sup> R. Pascu,<sup>1,2</sup> M. Danila,<sup>2</sup> and P. Godignon<sup>3</sup>

<sup>1</sup>*Electronics, Telecommunications and Information Technology, University Politehnica Bucharest, Bucharest 061071, Romania*

<sup>2</sup>*National Institute for Research and Development in Microtechnologies, Erou Iancu Nicolae Street 126A, 077190 Bucharest, Romania*

<sup>3</sup>*Centro Nacional de Microelectronica, C/del Til·lers. Campus Universitat Autònoma de Barcelona, 08193 Barcelona, Spain*

(Received 22 February 2015; accepted 23 June 2015; published online 2 July 2015)

Ni Schottky contacts on SiC have a nonideal behavior, with strong temperature dependence of the electrical parameters, caused by a mixed barrier on the contact area and interface states. A simple analytical model that establishes a quantitative correlation between Schottky contact parameter variation with temperature and barrier height non-uniformity is proposed. A Schottky contact surface with double Schottky barrier is considered. The main model parameters are the lower barrier ( $\Phi_{Bn,l}$ ) and a  $p$  factor which quantitatively evaluates the barrier non-uniformity on the Schottky contact area. The model is validated on Ni/4H-SiC Schottky contacts, post metallization sintered at high temperatures. The measured  $I_F$ - $V_F$ - $T$  characteristics, selected so as not to be affected by interface states, were used for model correlation. An inhomogeneous double Schottky barrier (with both nickel silicide and Ni droplets at the interface) is formed by a rapid thermal annealing (RTA) at 750 °C. High values of the  $p$  parameter are obtained from samples annealed at this temperature, using the proposed model. A significant improvement in the electrical properties occurs following RTA at 800 °C. The expansion of the Ni<sub>2</sub>Si phase on the whole contact area is evinced by an X-Ray diffraction investigation. In this case, the  $p$  factor is much lower, attesting the uniformity of the contact. The model makes it possible to evaluate the real Schottky barrier, for a homogenous Schottky contact. Using data measured on samples annealed at 800 °C, a true barrier height of around 1.73 V has been obtained for Ni<sub>2</sub>Si/4H-SiC Schottky contacts. © 2015 AIP Publishing LLC. [<http://dx.doi.org/10.1063/1.4923468>]

Since Ni is the most commonly used metal for Schottky contacts on SiC, it is essential to develop methods of improving its thermal reliability and electrical properties for high-power and high-temperature applications.<sup>1-10</sup> A rapid thermal annealing (RTA) at over 700 °C ensures a high Schottky barrier height (>1.7 V), required for elevated temperature operation.<sup>2,3</sup> Significant inhomogeneities, evinced by the temperature dependence of both ideality factor and barrier height, for the Ni/SiC contacts, were reported.<sup>1-10</sup> Most contacts are “multiphase,” causing the variations in barrier heights. Over the years, several models have emerged to incorporate inhomogeneity, including parallel conduction and Tung models.<sup>1,2,4,8-11</sup>

In this paper, an analytical macro model for Schottky contacts with barrier non-uniformities is developed. A parallel conduction on the contact surface, by means of two different Schottky barriers, is considered. A non-uniformity parameter is introduced to quantitatively characterize contact inhomogeneity. The model is proven on Ni/4H-SiC structures, annealed at 750 °C and 800 °C. The validity is confirmed by fitting the forward characteristics at temperatures up to 450 °C. The measurement of forward characteristics at high temperature is performed in order to minimize the effect of interface states.

The forward characteristics of a Schottky diode is usually described using the thermionic emission law with a single barrier and ideality factor. Thus, at low bias, where the

effect of the series resistance can be neglected, the forward current is given by<sup>1-10</sup>

$$I_F \cong I_S \exp\left(\frac{V_F}{nV_{th}}\right), \quad (1)$$

where  $n$  is the ideality factor and  $V_{th}$  is the thermal voltage.  $I_S$  is the saturation current which can be expressed as

$$I_S = A_n A_S T^2 \exp\left(-\frac{\Phi_{Bn,T}}{V_{th}}\right), \quad (2)$$

where  $A_S$  is the contact area and  $A_n$  is the Richardson constant for electrons (146 A/K<sup>2</sup>cm<sup>2</sup> for SiC).  $\Phi_{Bn,T}$  is the Schottky barrier at a given temperature or conventional barrier based on thermionic emission analysis.<sup>1</sup> A homogeneous Schottky contact has the same predictable (constant)  $\Phi_{Bn,T}$  and  $n$  at any temperature and voltage on the entire contact area.

A non-uniform Schottky contact includes two or more discrete barrier heights operating in parallel. Parallel conduction methodology began by challenging the notion that a single barrier height might exist for an entire interface.<sup>11</sup>

We propose a double-barrier Schottky contact model with two parallel diodes, suitable for non-uniform Ni Schottky contacts. After the sintering process at high temperatures, a non-uniform contact surface is obtained, with silicide zones having a high Schottky barrier and Ni zones with

a lower barrier. In this case, the saturation current has two components

$$\begin{aligned} I_S &= I_{S,l} + I_{S,h} \\ &= A_n A_{S,l} T^2 \exp\left(-\frac{\Phi_{Bn,l}}{V_{th}}\right) + A_n A_{S,h} T^2 \exp\left(-\frac{\Phi_{Bn,h}}{V_{th}}\right) \\ &= A_n A_S T^2 \exp\left(-\frac{\Phi_{Bn,l}}{V_{th}}\right) \left[ (1 - a_S) + a_S \exp\left(-\frac{\Delta\Phi_{Bn}}{V_{th}}\right) \right], \end{aligned} \quad (3)$$

where  $A_{S,l}$  and  $\Phi_{Bn,l}$  are the area and barrier height specific to the Ni-zone, while  $A_{S,h}$  and  $\Phi_{Bn,h}$  are their silicide-zone counterparts. The following normalizations in Eq. (3) are also used:

$$a_S = \frac{A_{S,h}}{A_S} \quad 1 - a_S = \frac{A_{S,l}}{A_S}. \quad (4)$$

The quantity  $\Delta\Phi_{Bn} = \Phi_{Bn,h} - \Phi_{Bn,l}$  assesses the difference between the model's Schottky barriers. Using (3) in (1) gives

$$\ln\left(\frac{I_F}{A_n A_S T^2}\right) = -\left(\frac{\Phi_{Bn,l}}{V_{th}} + p\right) + \frac{V_F}{nV_{th}}, \quad (5)$$

where

$$p = \ln\left[(1 - a_S) + a_S \exp\left(-\frac{\Delta\Phi_{Bn}}{V_{th}}\right)\right]^{-1}. \quad (6)$$

Comparing Eqs. (2) and (3) yields

$$\Phi_{Bn,T} = \Phi_{Bn,l} + pV_{th} = \Phi_{Bn,l} + \frac{k}{q}pT, \quad (7)$$

where  $k/q$  represents the ratio between the Boltzmann constant and elementary charge. Equation (7) evinces a slight linear increase of barrier height with temperature. This result is remarkable and can be expressed thus: any non-uniformity in the contact area will determine a temperature variation of the conventional Schottky barrier ( $\Phi_{Bn,T}$ ). For a uniform barrier contact,  $\Phi_{Bn,T}$  is close to  $\Phi_{Bn,l}$  and the temperature dependent term becomes negligible (in Eq. (7)). In this case, parameter  $p$  has a small value. Thus,  $p$  is a quantitative representation of non-uniformity in barrier height on the Schottky contact area. Furthermore, its introduction allows rapid assessment of conventional barrier temperature dependence.

The Schottky barrier can also be evaluated using the activation energy method. This technique is based on forward current variation versus temperature, at constant forward voltage. Using Eqs. (1)–(6) yields

$$\begin{aligned} \ln\left(\frac{I_F}{A_n A_S T^2}\right) &= \ln\left[(1 - a_S) + a_S \exp\left(-\frac{\Delta\Phi_{Bn}}{V_{th}}\right)\right] - \frac{E_A}{kT} \\ &= -p - \frac{E_A}{kT_0} \cdot \frac{T_0}{T}, \end{aligned} \quad (8)$$

where  $T_0$  is a reference temperature and

$$E_A = q\left(\Phi_{Bn,l} - \frac{V_F}{n}\right) \quad (9)$$

is the activation energy. By a linear fitting of  $\ln\left(\frac{I_F}{A_n A_S T^2}\right)$  as a function of the  $\frac{T_0}{T}$  ratio, the contact non-uniformity parameter ( $p$ ) and activation energy are determined. In Eq. (9),  $\Phi_{Bn,l}$ , the model's lower Schottky barrier is obtained using the ideality factor as input data. Since this parameter has a reduced variation range (between 1 and 1.13), any errors in extracted  $n$  will only slightly affect obtained barrier accuracy.

In order to validate the proposed double-barrier model, 2 batches of Schottky diodes have been fabricated. An  $n$ -doped 4H-SiC wafer with an epitaxial layer having 8  $\mu\text{m}$  thickness and  $10^{16} \text{ cm}^{-3}$  doping was used. A stack composed of Ni (150 nm) and Cr (10 nm) was deposited on the back-side for ohmic contact formation. A rapid thermal annealing was carried out, in Ar atmosphere, at 800 °C, for 5 min. On the front side, circular Schottky contacts of different diameters ( $D = 200, 300$ , and  $400 \mu\text{m}$ ) were defined in a  $\text{SiO}_2$  layer by a ramp etching, providing a uniform current distribution.<sup>6,7</sup> Afterwards, the same Ni (150 nm)/Cr (100 nm) ensemble has been deposited by sputtering in order to obtain the Schottky contact. A RTA was performed at  $T_A = 750^\circ\text{C}$  (batch B1) and 800 °C (batch B2) for 8 min, in a  $\text{N}_2$  atmosphere. Subsequently, Au layers were deposited on both wafer sides for packaging using wire bonding. The role of the Cr layer is to ensure the stability of the Schottky barrier by blocking the Au diffusion at high temperatures (over 400 °C). Some devices were encapsulated in a TO-39 package, as described in Refs. 6 and 7.

The  $I_F$ – $V_F$ – $T$  characteristics of the encapsulated devices have been measured at several temperatures up to 450 °C using a Keithley 4200 Semiconductor Characterization System.<sup>6,7</sup> Forward characteristics, of 3 samples selected from B1 and B2 batches, are depicted in Fig. 1. On a B2 sample (Fig. 1(a)), at low bias, an ideal exponential current increase is observed, for the entire measurement temperature range.

On another B2 diode (Fig. 1(b)), the characteristics at temperatures up to 150 °C exhibit two different slopes corresponding to different transport mechanisms.<sup>12</sup> The interface defects can be responsible for this behavior. The interface states play a major role in the charge transfer to or from the conduction band by capture and emission mechanisms or, with the metal, by tunneling.<sup>12</sup> This behavior is similar to that of a low-barrier Schottky contact. Interface states affect current conduction at low temperatures, only. At elevated temperatures, however, these states are partially or completely filled and their impact on current transport mechanisms is strongly diminished.<sup>12</sup> This means that the forward characteristics of the diode will once again become consistent with the thermionic emission law at high temperature. Clearly, on both B2 samples, the  $I_F$ – $V_F$  characteristics (Figs. 1(a) and 1(b)) measured at high temperature ( $>200^\circ\text{C}$ ) have an almost ideal behavior.

The characteristics of B1 diode (Fig. 1(c)) exhibit a lower voltage at the same current level and a higher series resistance than the sample of batch B2 (Fig. 1(b)), with identical contact diameter.

In order to prove the rectifying behavior of the investigated devices, the measured reverse characteristics for one

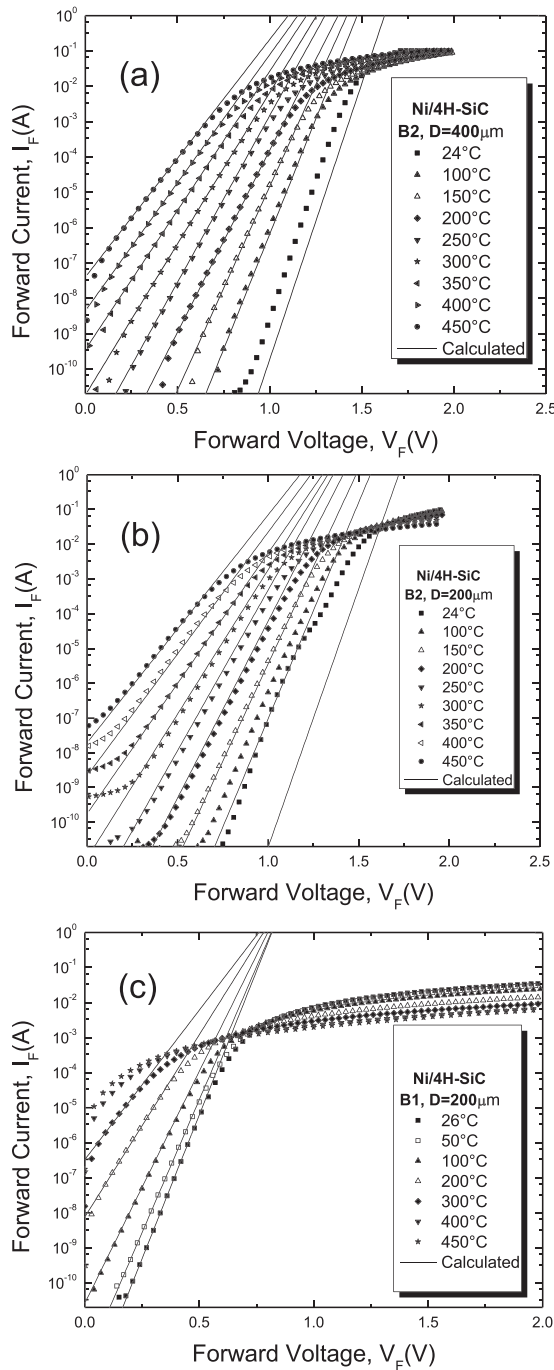


FIG. 1. Forward characteristics measured (symbols) and calculated using Eq. (5) (lines) of: two B2 samples ((a) and (b)) and a B1 sample (c).

of the samples are depicted in Fig. 2. The reverse current has a slight dependence of applied voltage and increases significantly with measurement temperature. The very low values of reverse current at room temperature are representative for SiC Schottky diodes.<sup>10</sup>

Based on measured  $I_F$ - $V_F$ - $T$  curves, the conventional Schottky barrier height and ideality factor have been extracted using Eqs. (1) and (2). In Fig. 3,  $\Phi_{Bn,T}$  and  $n$  versus measurement temperature are plotted. By annealing, Ni reacts with SiC by forming nickel silicides ( $\text{Ni}_{31}\text{Si}_{12}$  and  $\text{Ni}_2\text{Si}$ ). The improvement of the contact can be attributed to silicide formation, which consumes a surface SiC layer and creates a “new interface.”<sup>1</sup> Thus, reproducible  $I_F$ - $V_F$  characteristics (Figs. 1(a) and 1(b)) are obtained, on B2 samples

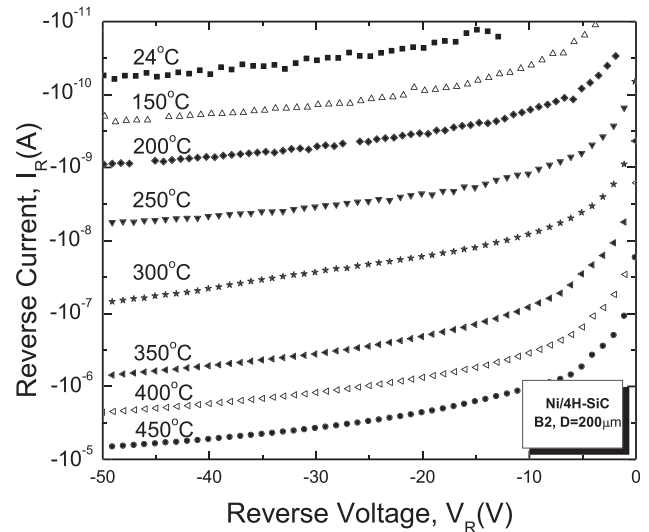


FIG. 2. Reverse characteristics measured at different temperatures on the B2 sample with forward curves from Fig. 1(b).

sintered at 800 °C. In this case, high values for the conventional Schottky barrier have been extracted (Fig. 3(a)), in good agreement with those reported in Ref. 4 on diodes annealed at 500 °C for 24 h. The ideality factor has a very low value ( $n < 1.05$ ), practically temperature independent for all measured samples.

A RTA at 750 °C was unable to determine Ni silicide formation on the entire contact area. Hence, the  $I_F$ - $V_F$ - $T$

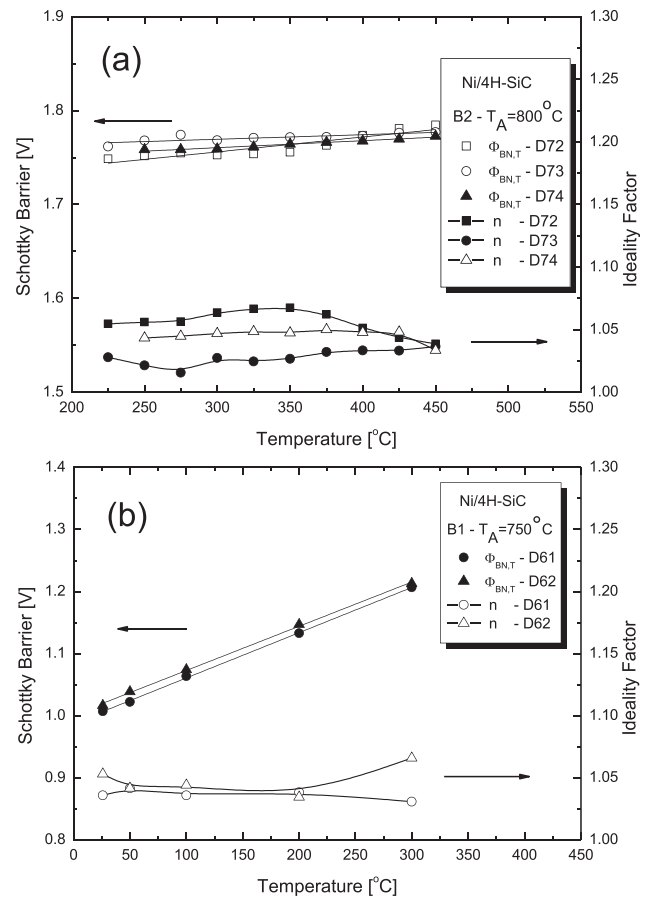


FIG. 3.  $\Phi_{Bn,T}$  and  $n$  versus measurement temperature for samples of batches: (a) B2 and (b) B1.

TABLE I. Double-barrier model parameters for several Ni/4H-SiC samples.

Sample	D ( $\mu\text{m}$ )	$p$ —Eq. (8)	$p$ —Eq. (10)	$\Phi_{Bn,l}$ (V)—Eq. (9)	$\Phi_{Bn,l}$ (V)—Eq. (7)
B2-D71	200	0.4–0.5	...	1.71	1.74
B2-D72	200	1.47–2.08	1.85	1.65–1.68	1.66
B2-D73	300	0.49–1.11	0.56	1.73	1.74
B2-D74	400	0.727–1.01	0.86	1.71–1.74	1.72
B1-D61	200	8.46–8.70	8.08	0.79	0.79
B1-D62	200	8.33–8.84	8.79	0.8	0.81

characteristics (Fig. 1(c)) and the conventional barrier heights (Fig. 3(b)) are strongly affected by the Ni patches on the Schottky surface. All devices from lot B1 exhibit much lower barrier than the values achieved on B2 samples (Fig. 3). In fact, it has been proven that even a very small fraction of the whole contact area covered by a low Schottky barrier is sufficient to rule conduction through the contact.<sup>2</sup> Due to the small value of the barrier, the exponential variation in forward characteristics of B1 samples occurs only up to 300 °C (Fig. 1(c)). Hence, the  $\Phi_{Bn,T}$  and  $n$  parameters for B1 structures can be extracted only up to this temperature (Fig. 3(b)).

The proposed macro-model has demonstrated that contact inhomogeneity leads to conventional barrier increase with temperature. The conventional barrier increases linearly with temperature, having a slope proportional with parameter  $p$  (see Eq. (7))

$$\frac{\Delta\Phi_{Bn,T}}{\Delta T} = \frac{k}{q} p T. \quad (10)$$

Thus, a considerable barrier variation with temperature indicates high contact non-uniformity. This analytic behavior was validated by the plots from Fig. 3.

Table I presents values obtained by fitting for the non-uniformity parameter ( $p$ ) from Eqs. (10) and (8), respectively. A good agreement between the values obtained with both techniques can be observed.

The high  $p$  values, achieved for lot B1 (annealed at 750 °C), confirm contact non-uniformity (Fig. 3(b)). The inhomogeneity is considerably reduced for B2 samples (Fig. 3(a)), as proven by the low  $p$  values (Table I).

After Ni annealing at 800 °C (batch B2), a thicker Ni<sub>2</sub>Si layer at the interface with SiC was identified by an X-Ray diffraction (XRD) analysis (Fig. 4). Because of the fixed low incidence angle ( $2\theta = 0.5^\circ$ ), all the surface of the sample is irradiated and thus an enhanced diffracted X-ray beam is collected at the detector from the whole sample surface.<sup>2–4</sup> A single phase composition, Ni<sub>2</sub>Si (the richest Ni content), was identified.

Table I also presents the model's barrier ( $\Phi_{Bn,l}$ ) obtained by extrapolation at 0 K in Eq. (7) and from Eq. (9).

Using the  $\Phi_{Bn,l}$  and  $p$  values from Table I in Eq. (5), the calculated  $I_F-V_F-T$  curves from Fig. 1 were plotted. A very good agreement between model curves and experimental data can be observed on the B2 samples at high measurement temperatures (over 200 °C—Figs. 1(a) and 1(b)). The discrepancies at lower temperature are caused by interface states, which were not considered in the proposed model. For the B1 sample, the model offers very good fitting of the

experimental data, even at low temperature (Fig. 1(c)). In this case, the interface states' influence is shunted by the double-barrier effect due to the very low value of one of the Schottky barriers ( $\Phi_{Bn,l} = 0.79$  V), corresponding to Ni/4H-SiC Schottky contacts.<sup>1,14</sup>

$\Phi_{Bn,l}$  values derived for all B2 structures (Table I) are close to the conventional Schottky barrier ( $\Phi_{Bn,T}$ , Fig. 2), for all measurement temperatures. The value obtained for  $\Phi_{Bn,T} \cong \Phi_{Bn,l} = 1.73$  V on B2 samples is the real barrier height of Ni<sub>2</sub>Si/4H-SiC Schottky contact.<sup>9</sup> Furthermore, this value is consistent with the theoretical amount for such contacts ( $\Phi_{Bn,T} \cong \Phi_{Ni_2Si} - \chi_{4H-SiC} \cong 1.7$  V).<sup>13</sup>

Table I presents the characteristics of two selected same diameter (200  $\mu\text{m}$ ) B2 samples. For D71, very low  $p$  values are obtained using Eq. (8), and around zero (not included in Table I), based on Eq. (10). This proves the high barrier uniformity on the entire Schottky contact area. In contrast, a slightly higher  $p$  and lower barrier are obtained on sample D72, indicating a degree of inhomogeneity, as can also be observed in Fig. 3(a).

For the B1 batch structures, a significant difference between  $\Phi_{Bn,T}$  and  $\Phi_{Bn,l}$  is evinced. This discrepancy occurs because of the Ni patches (with a barrier height—0.79 V—considerably smaller than that of Ni<sub>2</sub>Si), even though their effective surface is lower with many orders of magnitude than the total Schottky area. Therefore, an XRD analysis of sample D61 would not be able to identify the Ni patches. Conventional barrier extraction was performed considering the nominal contact area, which explains the differences between  $\Phi_{Bn,T}$  (Fig. 3(b)) and  $\Phi_{Bn,l}$  (Table I).

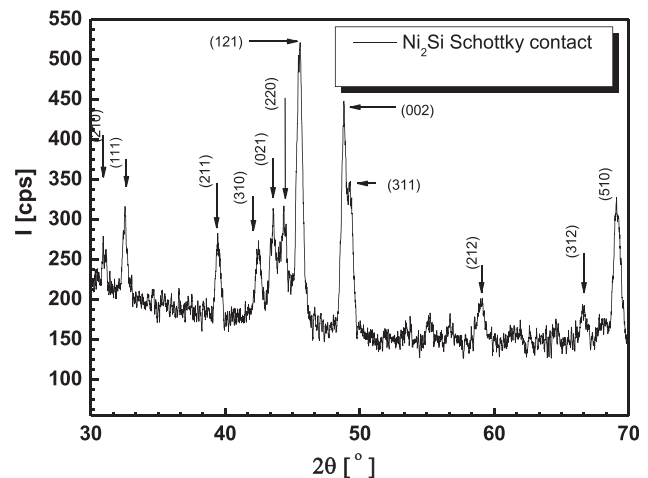


FIG. 4. XRD on a sample from batch B2, annealed at 800 °C.



In conclusion, a simple analytical model of a non-uniform Schottky contact was developed. In the model, parallel conduction through two Schottky barriers ( $\Phi_{Bn,h}$  and  $\Phi_{Bn,l}$ ) was considered. A model parameter ( $p$ ) was defined as a numerical depiction of the non-uniformity in Schottky barrier on the contact area.

The model was validated on Ni/4H-SiC Schottky diodes, annealed at 750 °C and 800 °C.  $I_F$ - $V_F$ - $T$  measured data are in good agreement with curves calculated from model equations. An annealing at 750 °C led to contact area inhomogeneity due to a distribution of low-barrier Ni patches embedded in the ideal, uniform, and high-barrier region. The Ni droplets, although covering an extremely low area, explain the high values ( $>8$ ) extracted for the  $p$  factor in this case.

A RTA at 800 °C determined the expansion of Ni<sub>2</sub>Si on essentially the entire area, resulting in a uniform and reproducible contact. The low values of non-uniformity parameter ( $p < 1$ ) and ideality factor ( $n < 1.05$ ) demonstrate the homogeneity of the Schottky contact. It should be noted that, for samples sintered at this high temperature, modeling was applied only to forward curves measured at over 200 °C, in order to minimize interface state effects. Furthermore, characterization on such a wide high-temperature range has proven that exemplary barrier uniformity can be reproducibly achieved on devices operating at over 200 °C.

The proposed model can be applied for other Schottky contacts on SiC such as Pt and Ti.

The research presented in this paper was supported by the PNII Romanian project under the Contract SiC-SET No.

21/ 2012. Also, the work has been funded by the Sectoral Operational Programme Human Resources Development 2007-2013 of the Ministry of European Funds through the Financial Agreement Nos. POSDRU/159/1.5/S/132395 and 134398.

- <sup>1</sup>P. M. Gammon, A. Pérez-Tomás, V. A. Shah, O. Vavasour, E. Donchev, J. S. Pang, M. Myronov, C. A. Fisher, M. R. Jennings, D. R. Leadley, and P. A. Mawby, *J. Appl. Phys.* **114**, 223704 (2013).
- <sup>2</sup>F. Roccaforte, F. La Via, A. Baeri, V. Raineri, L. Calcagno, and F. Mangano, *J. Appl. Phys.* **96**, 4313 (2004).
- <sup>3</sup>V. Kumar, A. S. Maan, and J. Akhtar, *J. Vac. Sci. Technol. B* **32**, 041203 (2014).
- <sup>4</sup>T. N. Oder, T. L. Sung, M. Barlow, J. R. Williams, A. C. Ahyi, and T. Isaacs-Smith, *J. Electron. Mater.* **38**, 772 (2009).
- <sup>5</sup>A. M. Enver, Y. Nezir, and T. Abdulmecit, *J. Appl. Phys.* **102**, 043701 (2007).
- <sup>6</sup>G. Brezeanu, F. Draghici, M. Badila, F. Craciunoiu, G. Pristavu, R. Pascu, and F. Bernea, *Mater. Sci. Forum* **778–780**, 1063 (2014).
- <sup>7</sup>R. Pascu, G. Pristavu, G. Brezeanu, F. Draghici, M. Badila, and F. Craciunoiu, *Mater. Sci. Forum* **121–123**, 436 (2015).
- <sup>8</sup>M. Vivona, K. Alassaad, V. Souliere, F. Giannazzo, F. Roccaforte, and G. Ferro, *Mater. Sci. Forum* **778–780**, 706 (2014).
- <sup>9</sup>F. Roccaforte, F. Giannazzo, F. Iucolano, J. Eriksson, M. H. Weng, and V. Raineri, *Appl. Surf. Sci.* **256**, 5727–5735 (2010).
- <sup>10</sup>F. Roccaforte, F. La Via, V. Raineri, R. Pierobon, and E. Zanoni, *J. Appl. Phys.* **93**, 9137 (2003).
- <sup>11</sup>I. Ohdomari and K. N. Tu, *J. Appl. Phys.* **51**, 3735 (1980).
- <sup>12</sup>A. Ahaitouf, H. Srour, S. Ould Saad Hamady, N. Fressengeas, A. Ougazzaden, and J. P. Salvestrini, *Thin Solid Films* **522**, 345 (2012).
- <sup>13</sup>J. A. Kittl, M. A. Pawlak, A. Lauwers, C. Demeurisse, K. Opsomer, K. Anil, C. Vrancken, M. Van Dal, A. Veloso, S. Kubicek *et al.*, *IEEE Electron Device Lett.* **27**, 34 (2006).
- <sup>14</sup>D. J. Ewing, L. M. Porter, Q. Wahab, X. Ma, T. S. Sudharshan, S. Tumakha, M. Gao, and L. J. Brillson, *J. Appl. Phys.* **101**, 114514 (2007).